



ADAPTATION TO CLIMATE CHANGE IN THE NILE DELTA THROUGH INTEGRATED COASTAL ZONE MANAGEMENT PROJECT

**INTEGRATED COASTAL ZONE MANAGEMENT IN THE  
NORTHERN COAST OF EGYPT  
– A SCOPING STUDY –**

**ANNEX I:**

**ANNEX I: HAZARD CHARACTERIZATION AND CLIMATE CHANGE**

**DECEMBER 2016**





## INDEX

ANNEX I: HAZARD CHARACTERIZATION AND CLIMATE CHANGE .....	AI.1
1. INTRODUCTION .....	AI.1
2. HISTORICAL CHARACTERIZATION OF CLIMATIC DRIVERS .....	AI.1
2.1. Waves: GOW database (spatial resolution: 0.125°).....	AI.1
2.2. Storm surge: GOS database (spatial resolution: 0.064° x 0.114°).....	AI.3
2.3. Sea surface temperature: GRHSST database (spatial resolution: 0.05°).....	AI.3
2.4. Air temperature: Seawind II database (spatial resolution: 0.125°).....	AI.4
2.5. Precipitation: Seawind II database (spatial resolution: 0.125°).....	AI.4
3. NEAR- AND LONG-TERM PROJECTIONS OF CLIMATIC DRIVERS.....	AI.6
3.1. Waves: GOW projections (spatial resolution: 0.125°) .....	AI.6
3.2. Storm surge: GOS projections (spatial resolution: 0.064° x 0.114°) .....	AI.8
3.3. Sea level rise: Slangen et al. (2014) (spatial resolution: 1°).....	AI.8
3.4. Sea surface temperature: CMIP5 (spatial resolution: 1°) .....	AI.10
3.5. Air temperature: CMIP5 (spatial resolution: 1°) .....	AI.12
3.6. Precipitation: CMIP5 (spatial resolution: 1°).....	AI.15



## ANNEX I: HAZARD CHARACTERIZATION AND CLIMATE CHANGE

### 1. INTRODUCTION

This annex presents the detailed information concerning the climate data used in the project Integrated Coastal Zone Management in Egypt - A Scoping Study. One of the main efforts made in this work consisted in describing the hazard, herein characterized by historical information and future projections of climatic drivers. They include waves, storm surge, sea level, sea surface temperature, air temperature and precipitation. Its analysis allows the definition of climatic conditions at different time horizons and assessments: historical, present, near-term prediction or climatic projections throughout the 21<sup>st</sup> century.

The results of the climate drivers are given along the Egyptian Northern Coast in the different coastal points previously defined (every 10 km). The Egyptian northern coastline is indicated in each figure and is referenced by its longitude (x-axis) and latitude (y-axis).

### 2. HISTORICAL CHARACTERIZATION OF CLIMATIC DRIVERS

The historical characterization of the climatic drivers allows to assess how they have changed over the last decades and how they have contributed to coastal impacts.

#### 2.1. Waves: GOW database (spatial resolution: 0.125°)

The GOW (Global Ocean Waves) database comprises hourly data of waves with a spatial resolution of 0.125° for the period 1979-2015 (Reguero et al., 2012). The following figures show the spatial variability of wave statistics along the Egyptian coast.

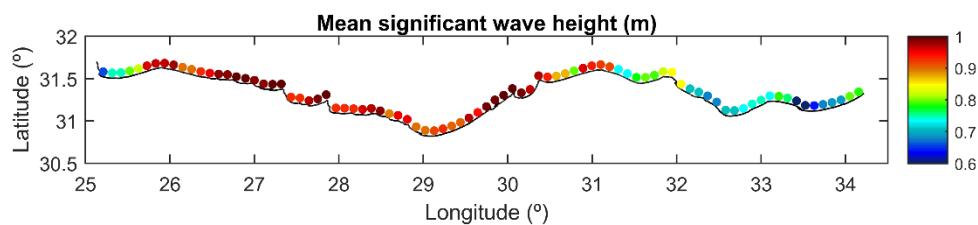


Fig. 1 Mean value of the hourly mean significant wave height (m) for the period 1979-2015

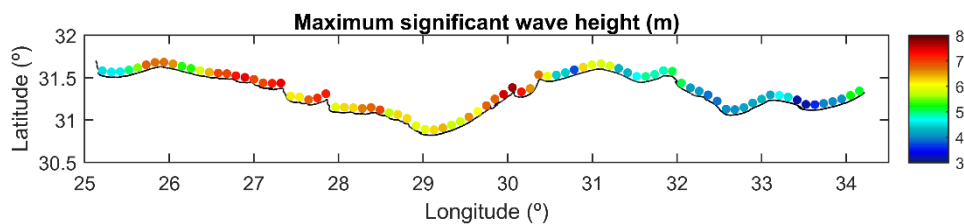


Fig. 2 Maximum value of the hourly mean significant wave height (m) for the period 1979-2015

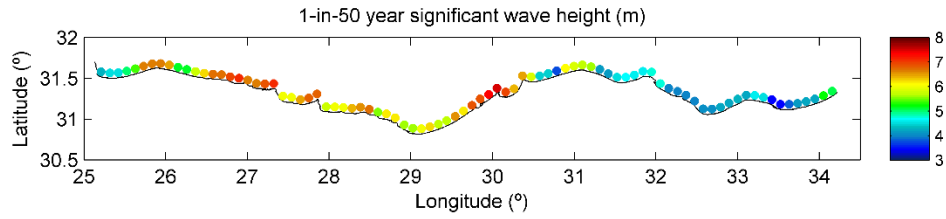


Fig. 3 1-in-50 year significant wave height (m) for the period 1979-2015

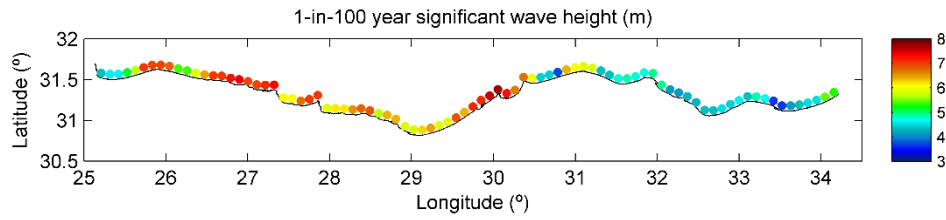


Fig. 4 1-in-100 year significant wave height (m) for the period 1979-2015

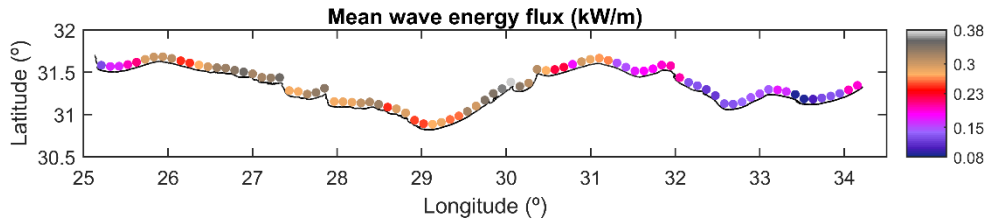


Fig. 5 Mean value of the wave energy flux (kW/m) for the period 1979-2015

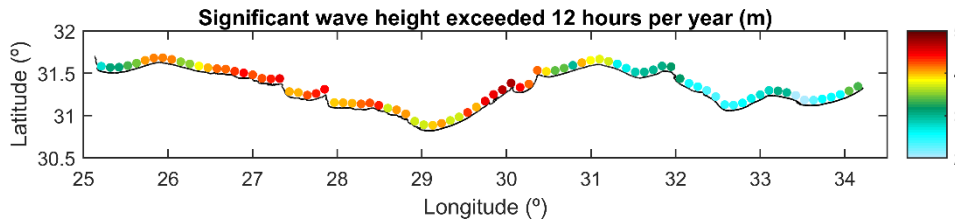


Fig. 6 Mean value of the significant wave height only exceeded 12 hours per year (m) for the period 1979-2015

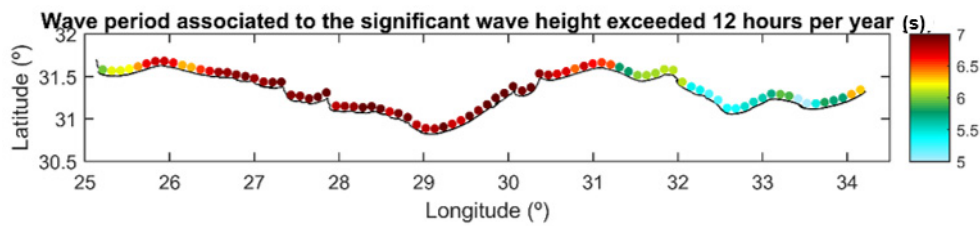


Fig. 7 Value of the wave period associated to the significant wave height exceeded 12 hours per year (s) for the period 1979-2015

## 2.2. Storm surge: GOS database (spatial resolution: 0.064° x 0.114°)

The GOS (Global Ocean Surges) database comprises hourly data of storm surge with a spatial resolution of 0.064° x 0.114° for the period 1979-2014 (Cid et al., 2014). The following figure show the spatial variability of the 99<sup>th</sup> percentile of storm surge along the Egyptian coast.

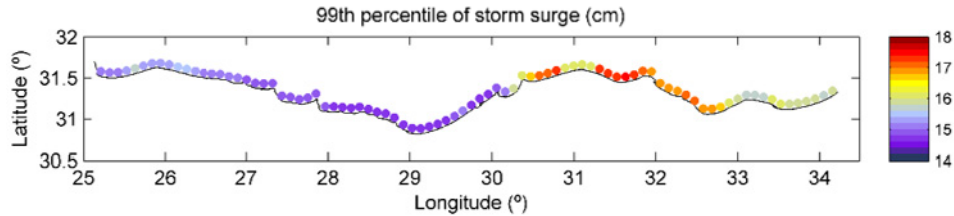


Fig. 8 Value of the 99 percentile of storm surge (cm) for the period 1975-2015

## 2.3. Sea surface temperature: GRHSST database (spatial resolution: 0.05°)

The GRHSST (Group for High Resolution Sea Surface Temperature) database comprises hourly data of sea surface temperature with a spatial resolution of 0.05° for the period 1985-2015 (Robert-Jones et al., 2012). The following figures show the spatial variability of the minimum, mean and maximum values of sea surface temperature along the Egyptian coast.

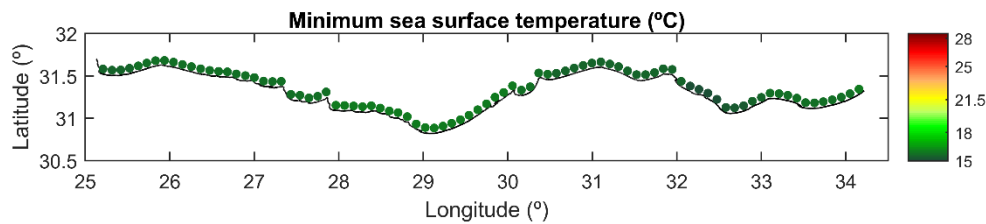


Fig. 9 Minimum value of the sea surface temperature (°C) for the period 1985-2015

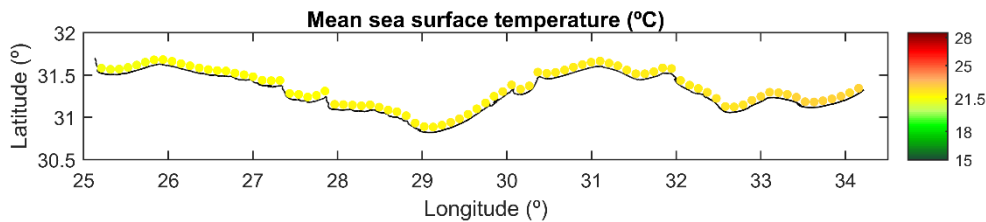


Fig. 9 Mean value of the sea surface temperature (°C) for the period 1985-2015

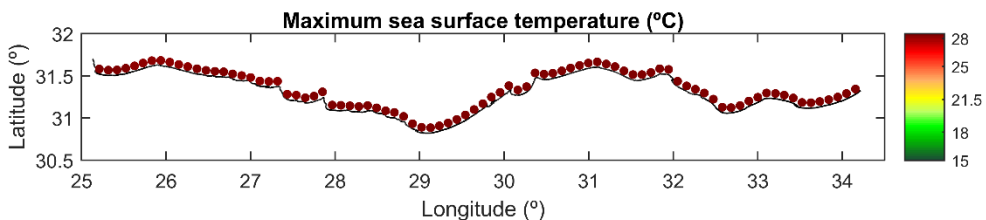


Fig. 10 Maximum value of the sea surface temperature (°C) for the period 1985-2015

## 2.4. Air temperature: Seawind II database (spatial resolution: 0.125°)

The Seawind II database comprises hourly data of air temperature with a spatial resolution of 0.125° for the period 1989-2015 (Donlon et al., 2012). The following figures show the spatial variability of the mean monthly values of the minimum, mean and maximum air temperature along the Egyptian coast. Please, note that air temperature data are obtained from the ocean model and consequently can be considered as a lower limit.

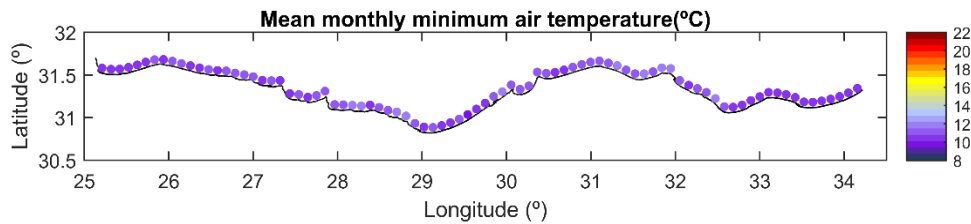


Fig. 11 Mean value of the monthly minimum air temperature (°C) for the period 1989-2015

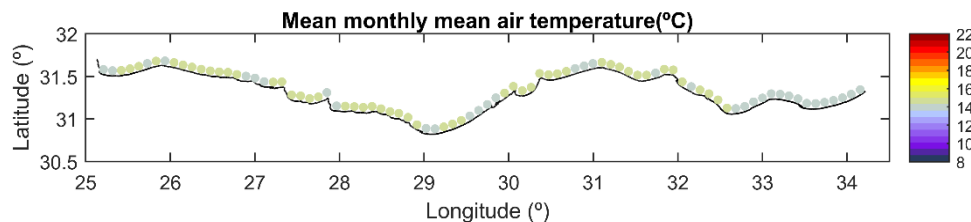


Fig. 12 Mean value of the monthly mean air temperature (°C) for the period 1989-2015

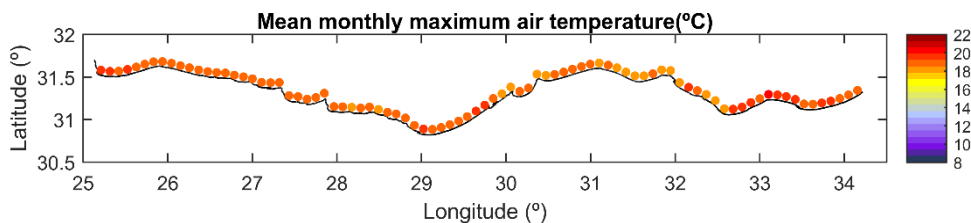


Fig. 13 Mean value of the monthly maximum air temperature (°C) for the period 1989-2015

## 2.5. Precipitation: Seawind II database (spatial resolution: 0.125°)

The Seawind II database comprises hourly data of precipitation with a spatial resolution of 0.125° for the period 1989-2015. The following figures show the spatial variability of the annual mean precipitation, the validation of the Seawind II dataset in Alexandria and Marsa Matrouh with GHCN (Global Historical Climatology Network - Daily) data to demonstrate its good performance along the Egyptian coast, and the monthly mean value of precipitation during wet and dry seasons (April to September and October to March, respectively).

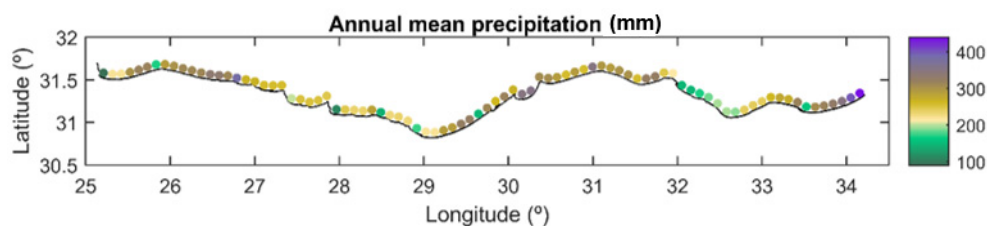


Fig. 14 Mean value of the annual precipitation (mm) for the period 1989-2015

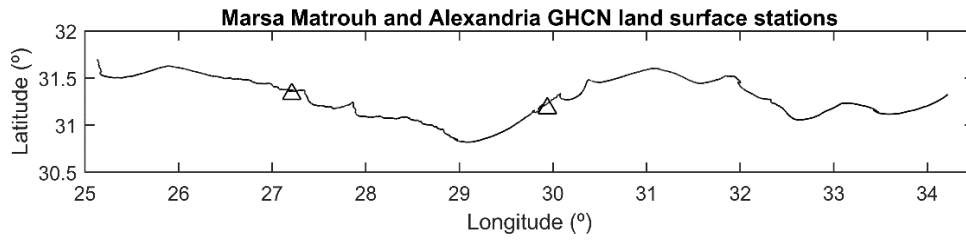


Fig. 15 Location of Marsa Matrouh and Alexandria GHCN land surface stations

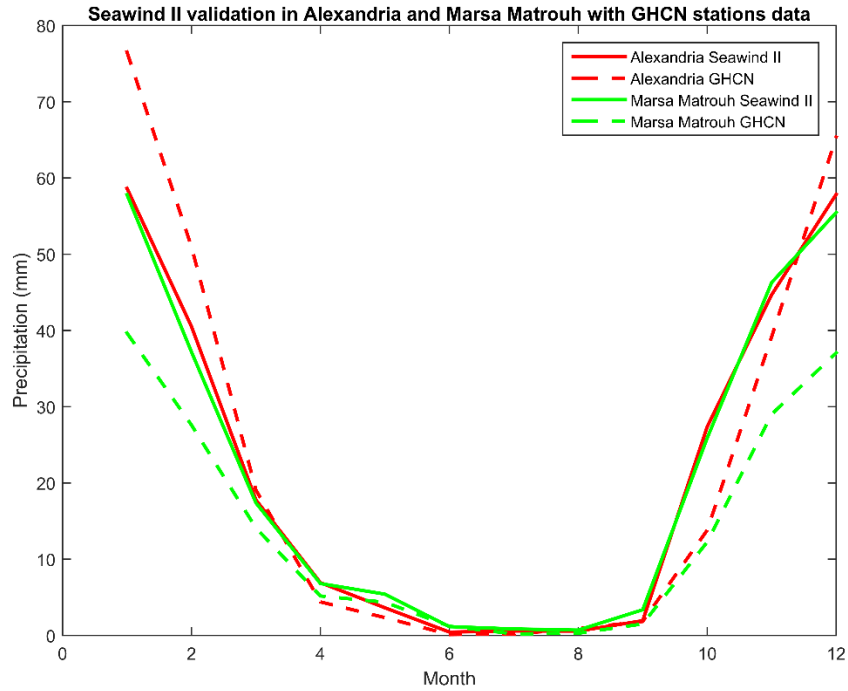


Fig. 16 Seawind II validation in Marsa Matrouh and Alexandria GHCN stations with GHCN data

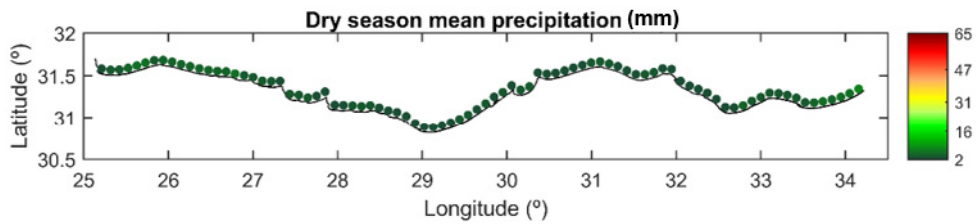


Fig. 17 Monthly mean value of precipitation (mm) during dry season (April to September) for the period 1989-2015

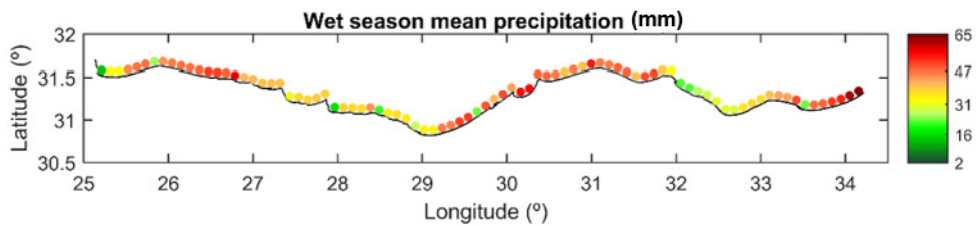


Fig. 19 Monthly mean value of precipitation (mm) during dry season (October to March) for the period 1989-2015

### 3. NEAR- AND LONG-TERM PROJECTIONS OF CLIMATIC DRIVERS

The way the atmosphere will behave under different climate change scenarios is derived by global circulation models (GCM). GCMs are numerical models that represent physical processes in the atmosphere, ocean, cryosphere and land surface and are the most advanced tools currently available for simulating the response of the global climate system to increasing greenhouse gas concentrations (IPCC, 2013). Herein climate driver projections derived from GCMs are presented for the near- and long-term, and under two Representative Concentration Pathways (RCP) scenarios based on Greenhouse gas (GHG) emissions: RCP4.5, corresponding to a pathway with moderate GHG emissions; and RCP8.5, that accounts for the pathway with the highest GHG emissions.

#### 3.1. Waves: GOW projections (spatial resolution: 0.125°)

Wave statistics projections have been developed at a spatial resolution of 0.125° (Perez et al., 2015) using 17 GCMs from the Coupled Model Intercomparison Project Phase 5 (CMIP5, Taylor et al., 2012). The following figures show the results for the RCP4.5 and RCP8.5 scenarios, and for the periods 2010-2039 and 2040-2069 with respect to the reference period 1975-2004.

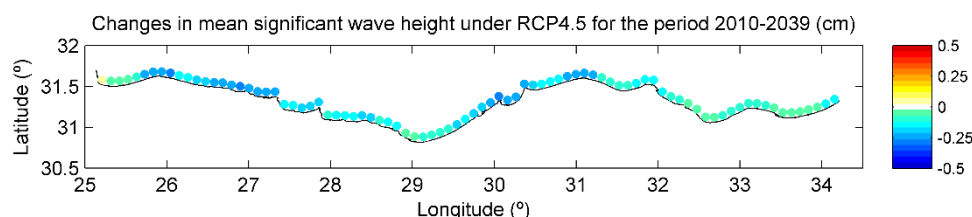


Fig. 18 Changes in the mean value of the significant wave height (cm) under RCP4.5 for the period 2010-2039 with respect to the reference period 1975-2004

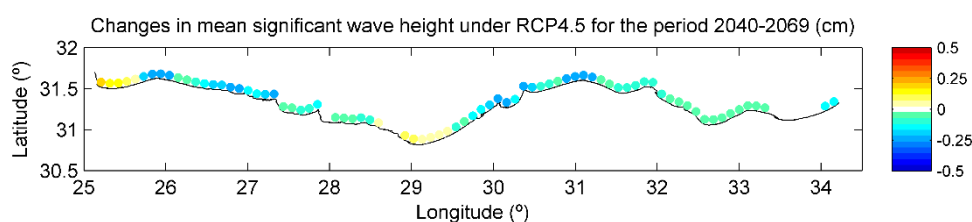


Fig. 19 Changes in the mean value of the significant wave height (cm) under RCP4.5 for the period 2040-2069 with respect to the reference period 1975-2004

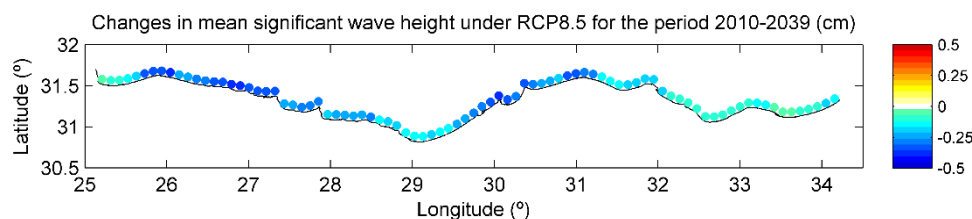


Fig. 20 Changes in the mean value of the significant wave height in (cm) under RCP8.5 for the period 2010-2039 with respect to the reference period 1975-2004

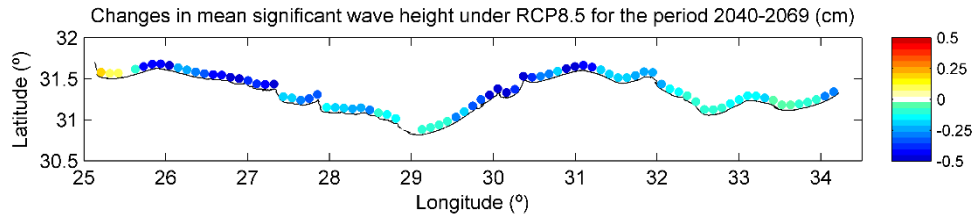


Fig. 21 Changes in the mean value of the significant wave height in (cm) under RCP8.5 for the period 2040-2069 with respect to the reference period 1975-2004

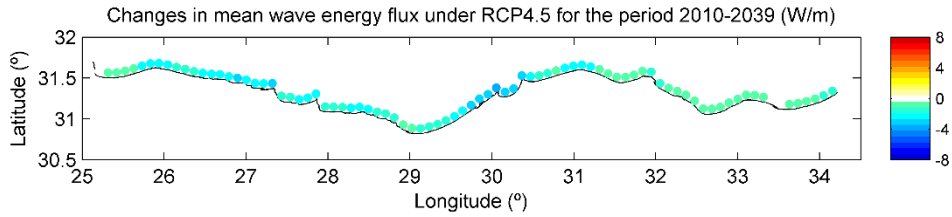


Fig. 22 Changes in the mean value of the wave energy flux (W/m) under RCP4.5 for the period 2010-2039 with respect to the reference period 1975-2004

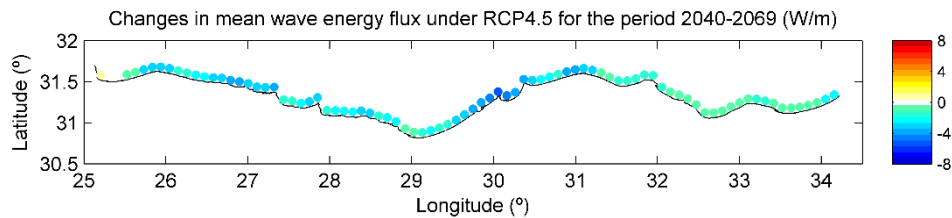


Fig. 23 Changes in the mean value of the wave energy flux (W/m) under RCP4.5 for the period 2040-2069 with respect to the reference period 1975-2004

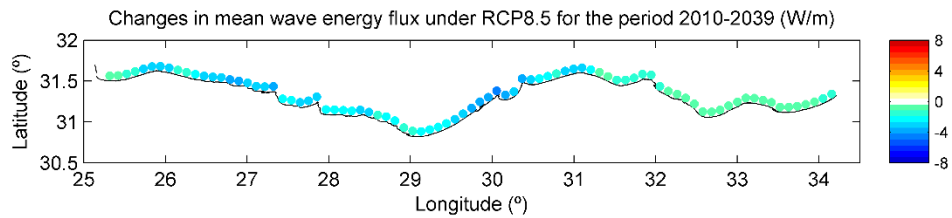


Fig. 24 Changes in the mean value of the wave energy flux (W/m) under RCP8.5 for the period 2010-2039 with respect to the reference period 1975-2004

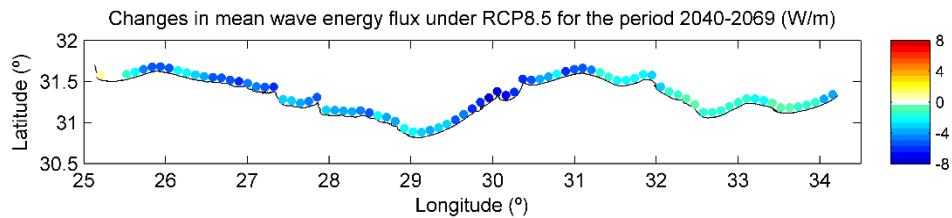


Fig. 25 Changes in the mean value of the wave energy flux (W/m) under RCP4.5 for the period 2040-2069 with respect to the reference period 1975-2004

### 3.2. Storm surge: GOS projections (spatial resolution: 0.064° x 0.114°)

The storm surge projections have been developed at a spatial resolution of 0.064° x 0.114° using 6 GCMs from the CMIP5 (Taylor et al., 2012). The following figures show the 99<sup>th</sup> percentile of storm surge projected for the RCP4.5 and RCP8.5 emission scenarios, and for the period 2070-2099 with respect to the reference period 1975-2004. Results for the near term are not available.

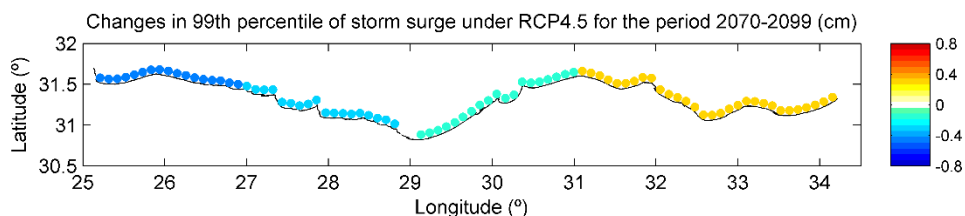


Fig. 26 Changes in the 99<sup>th</sup> percentile of storm surge (m) under RCP4.5 for the period 2070-2099 with respect to the reference period 1975-2004

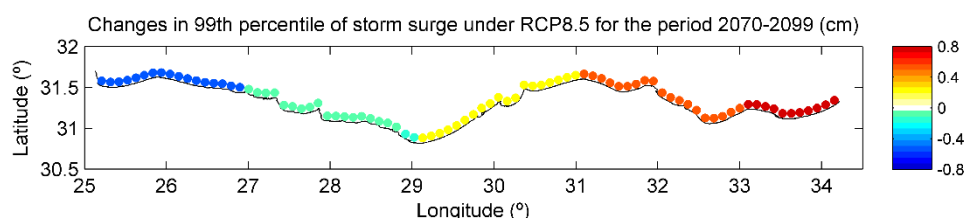


Fig. 29 Changes in the 99<sup>th</sup> percentile of storm surge (m) under RCP8.5 for the period 2070-2099 with respect to the reference period 1975-2004

### 3.3. Sea level rise: Slangen et al. (2014) (spatial resolution: 1°)

Slangen et al. (2014) developed the regionalized global sea-level projections in all the basins around the world at a spatial resolution of 1°. They have been developed under the RCP4.5 and RCP8.5 scenarios and for the period 2081-2100 with respect to the reference period 1985-2005. Using the global mean values of sea level rise provided by the IPCC (Church et al., 2013) over the 21<sup>st</sup> century and assuming the same spatial distribution patterns of the regionalized global sea-level projections for the end of the century, regional sea level rise for the periods 2016-2035 and 2040-2069 have been herein derived. The following figures show sea-level rise projections for the RCP4.5 and RCP8.5 emission scenarios, and for the periods 2016-2035, 2046-2065 and 2081-2100, with respect to the reference period 1985-2005.

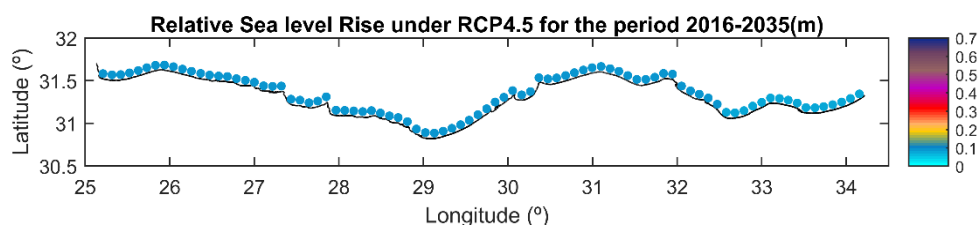


Fig. 27 Relative sea level rise (m) under RCP4.5 for the period 2016-2035 with respect to to the reference period 1986-2005

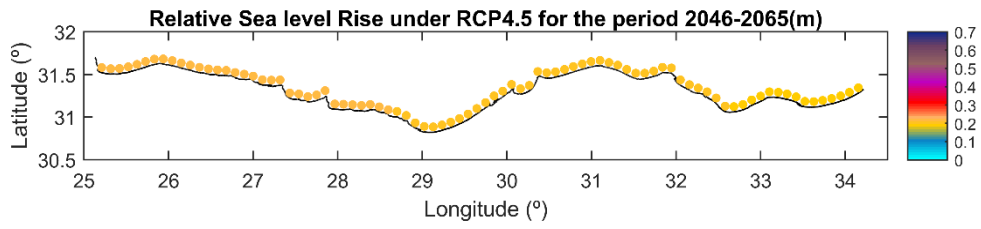


Fig. 28 Relative sea level rise (m) under RCP4.5 for the period 2046-2065 with respect to to the reference period 1986-2005

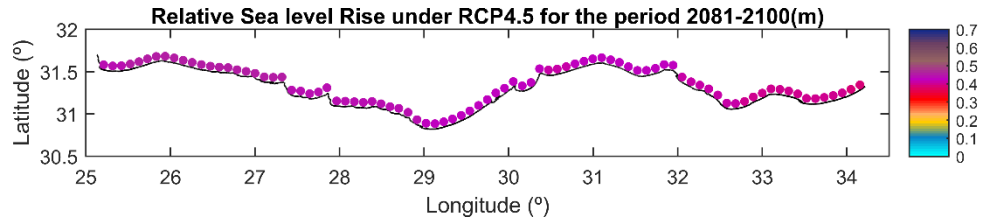


Fig. 29 Relative sea level rise (m) under RCP4.5 for the period 2081-2100 with respect to to the reference period 1986-2005

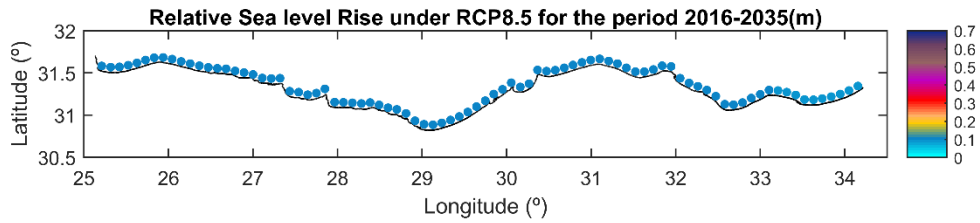


Fig. 30 Relative sea level rise (m) under RCP8.5 for the period 2016-2035 with respect to to the reference period 1986-2005

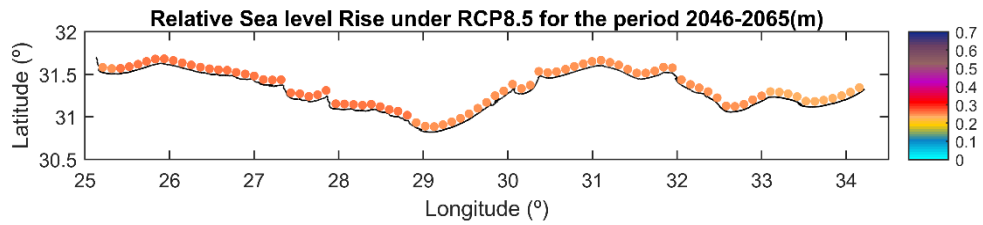


Fig. 31 Relative sea level rise (m) under RCP8.5 for the period 2046-2065 with respect to to the reference period 1986-2005

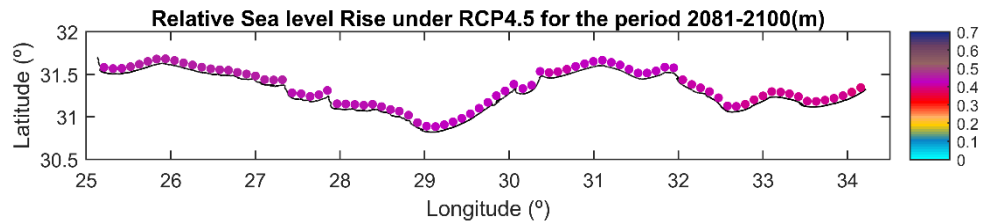


Fig. 32 Relative sea level rise (m) under RCP8.5 for the period 2081-2100 with respect to to the reference period 1986-2005

### 3.4. Sea surface temperature: CMIP5 (spatial resolution: 1°)

Sea surface temperature projections have been assembled using the results given by the CMIP5 models at a spatial resolution of 1° (Taylor et al., 2012). The following figures show changes in the minimum, mean and maximum values of sea surface temperature for the RCP4.5 and RCP8.5 emission scenarios, and for the periods 2030-2040 (near-term) and 2050-2070 (long-term) with respect to the period 1986-2005.

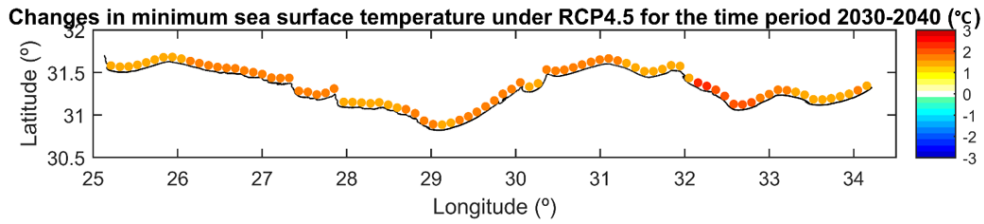


Fig. 33 Changes in the minimum sea surface temperature (°C) under RCP4.5 for the period 2030-2040 with respect to the reference period 1986-2005

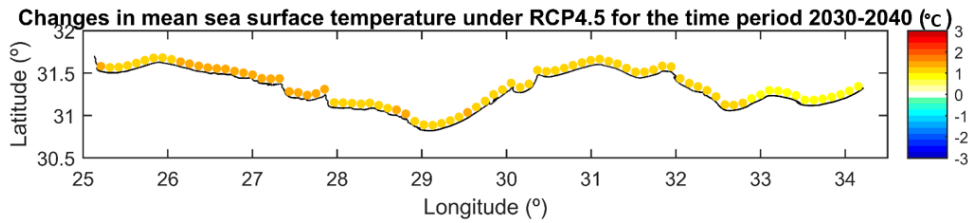


Fig. 34 Changes in the mean sea surface temperature (°C) under RCP4.5 for the period 2030-2040 with respect to the reference period 1986-2005

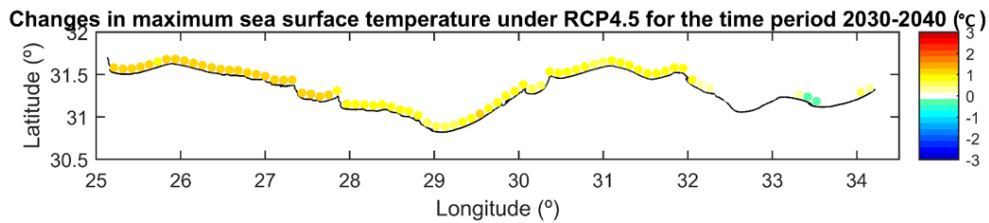


Fig. 35 Changes in the maximum sea surface temperature (°C) under RCP4.5 for the period 2030-2040 with respect to the reference period 1986-2005

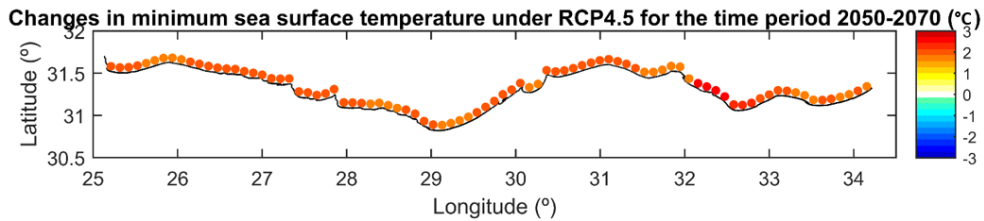


Fig. 39 Changes in the minimum sea surface temperature (°C) under RCP4.5 for the period 2050-2070 with respect to the reference period 1986-2005

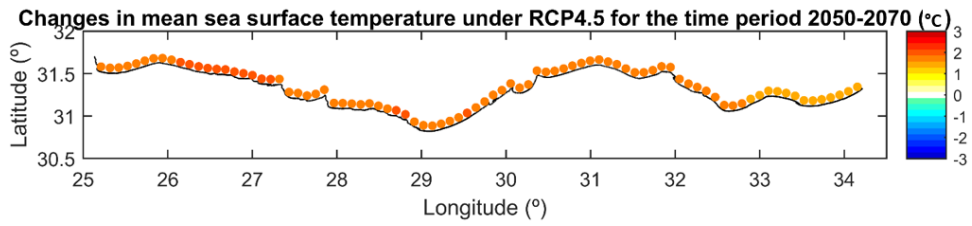


Fig. 36 Changes in the mean sea surface temperature (°C) under RCP4.5 for the period 2050-2070 with respect to the reference period 1986-2005

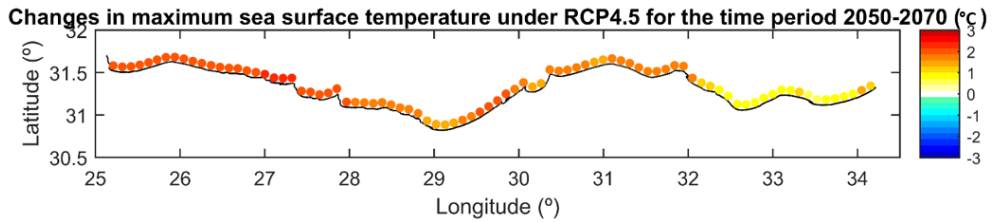


Fig. 37 Changes in the maximum sea surface temperature (°C) under RCP4.5 for the period 2050-2070 with respect to the reference period 1986-2005

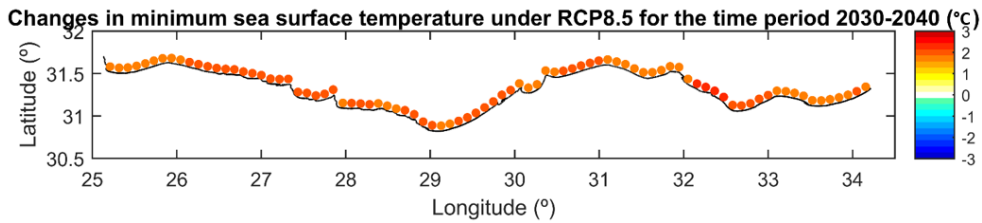


Fig. 38 Changes in the minimum sea surface temperature (°C) under RCP8.5 for the period 2030-2040 with respect to the reference period 1986-2005

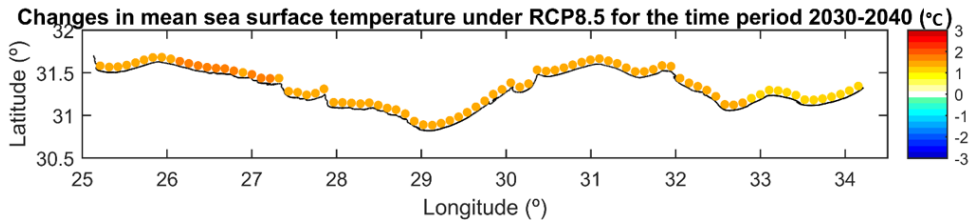


Fig. 39 Changes in the mean sea surface temperature (°C) under RCP8.5 for the period 2030-2040 with respect to the reference period 1986-2005

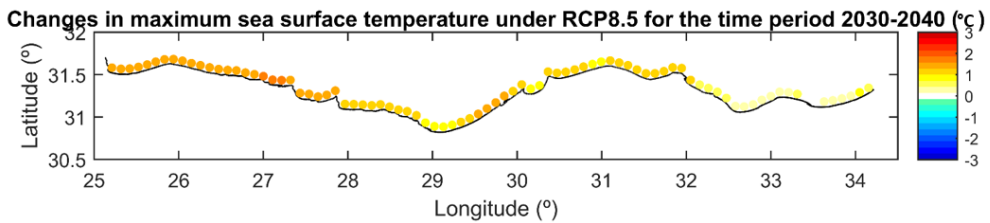


Fig. 40 Changes in the maximum sea surface temperature (°C) under RCP8.5 for the period 2030-2040 with respect to the reference period 1986-2005

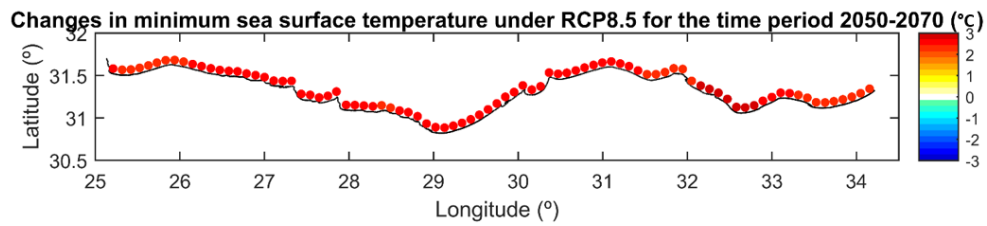


Fig. 41 Changes in the minimum sea surface temperature (°C) under RCP8.5 for the period 2050-2070 with respect to the reference period 1986-2005

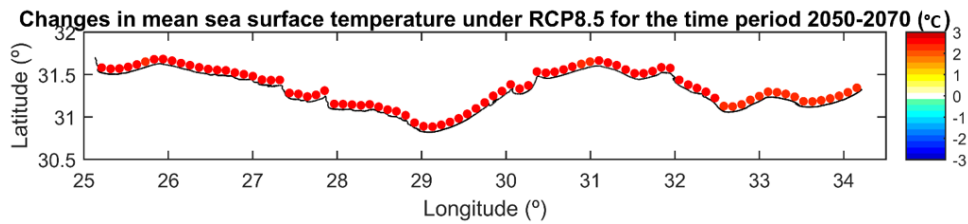


Fig. 42 Changes in the mean sea surface temperature (°C) under RCP8.5 for the period 2050-2070 with respect to the reference period 1986-2005

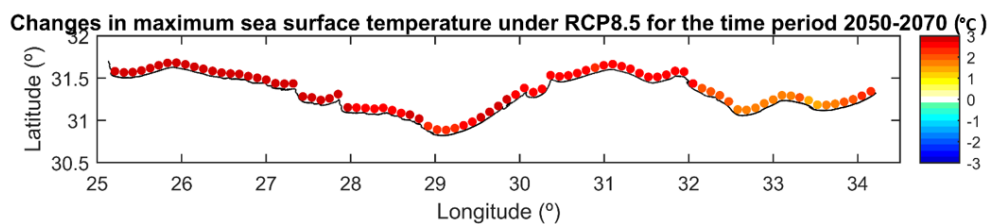


Fig. 43 Changes in the maximum sea surface temperature (°C) under RCP8.5 for the period 2050-2070 with respect to the reference period 1986-2005

### 3.5. Air temperature: CMIP5 (spatial resolution: 1°)

Air temperature projections have been assembled using the results given by the CMIP5 models at a spatial resolution of 1° (Taylor et al., 2012). The following figures show changes in the mean value of the monthly minimum, mean and maximum air temperatures for the RCP4.5 and RCP8.5 emission scenarios, and for the periods 2030-2040 and 2050-2070 with respect to the reference period 1986-2005. Please, note that air temperature projections are obtained from the ocean model and consequently can be considered as a lower limit of the projections.

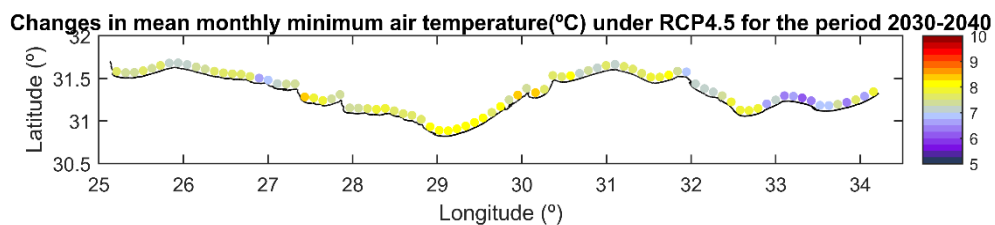


Fig. 44 Changes in the mean value of the monthly minimum air temperature (°C) under RCP4.5 for the period 2030-2040 with respect to the reference period 1986-2005

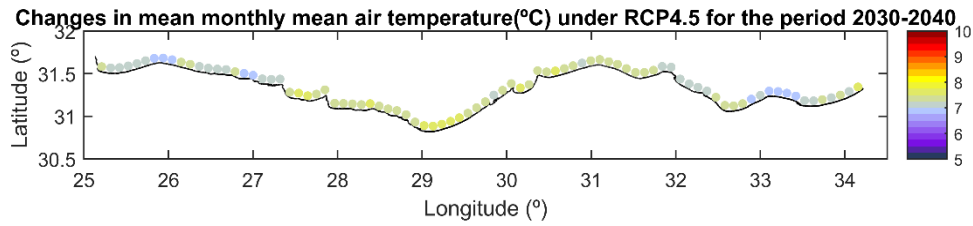


Fig. 49 Changes in the mean value of the monthly mean air temperature (°C) under RCP4.5 for the period 2030-2040 with respect to the reference period 1986-2005

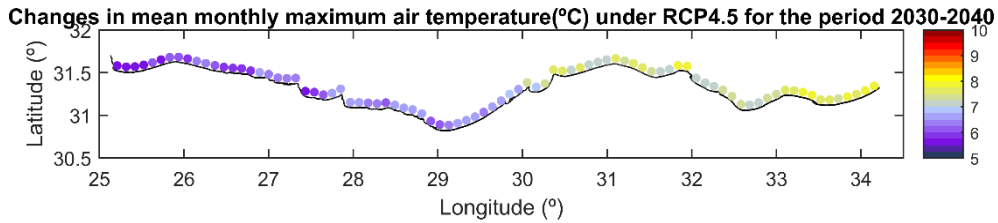


Fig. 45 Changes in the mean value of the monthly maximum air temperature (°C) under RCP4.5 for the period 2030-2040 with respect to the reference period 1986-2005

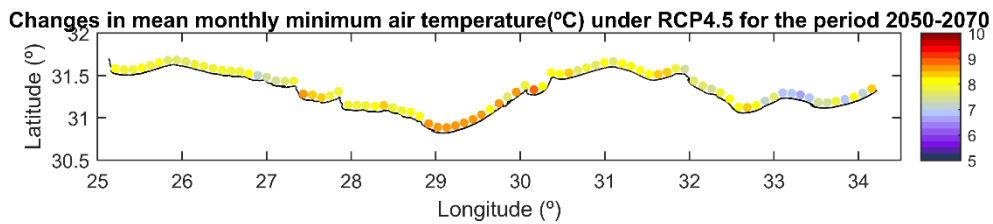


Fig. 46 Changes in the mean value of the monthly minimum air temperature (°C) under RCP4.5 for the period 2050-2070 with respect to the reference period 1986-2005

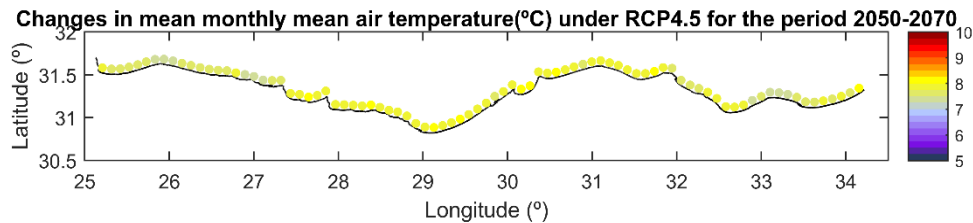


Fig. 47 Changes in the mean value of the monthly mean air temperature (°C) under RCP4.5 for the period 2050-2070 with respect to the reference period 1986-2005

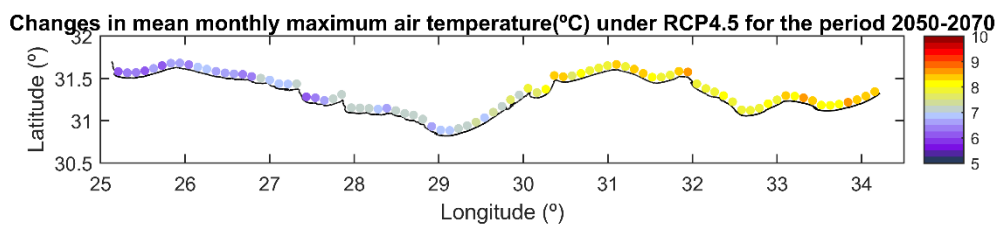


Fig. 48 Changes in the mean value of the monthly maximum air temperature (°C) under RCP4.5 for the period 2050-2070 with respect to the reference period 1986-2005

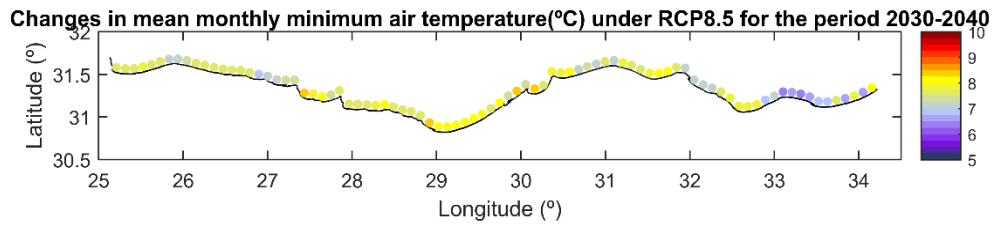


Fig. 49 Changes in the mean value of the monthly minimum air temperature (°C) under RCP8.5 for the period 2030-2040 with respect to the reference period 1986-2005

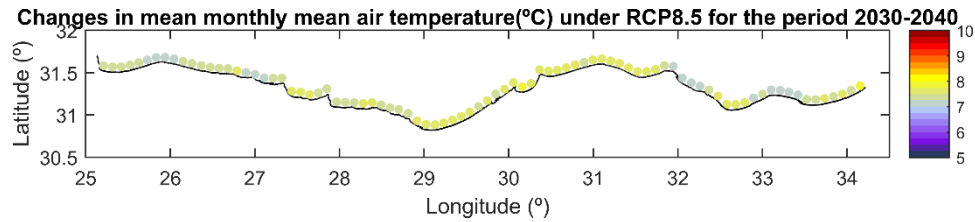


Fig. 50 Changes in the mean value of the monthly mean air temperature (°C) under RCP8.5 for the period 2030-2040 with respect to the reference period 1986-2005

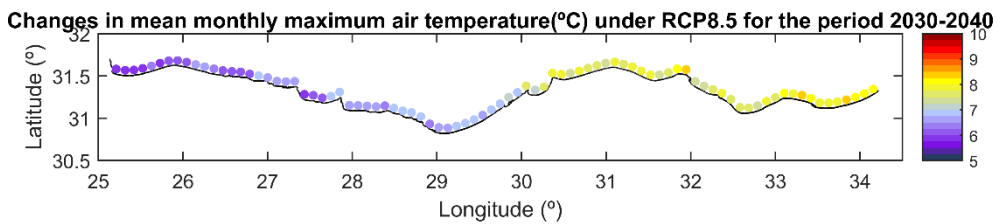


Fig. 51 Changes in the mean value of the monthly maximum air temperature (°C) under RCP8.5 for the period 2030-2040 with respect to the reference period 1986-2005

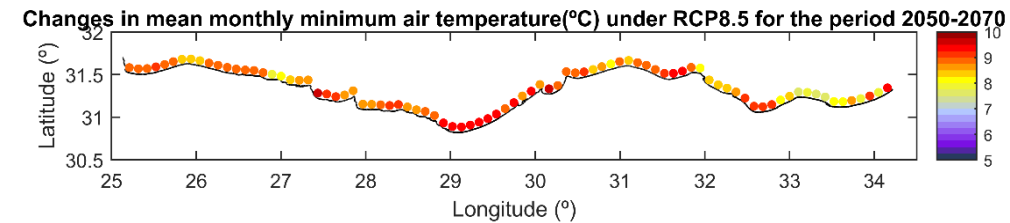


Fig. 52 Changes in the mean value of the monthly minimum air temperature (°C) under RCP8.5 for the period 2050-2070 with respect to the reference period 1986-2005

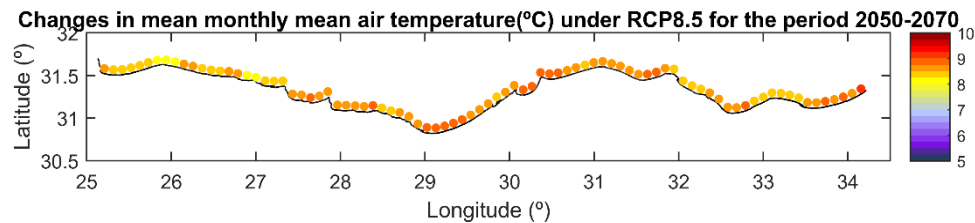


Fig. 53 Changes in the mean value of the monthly mean air temperature (°C) under RCP8.5 for the period 2050-2070 with respect to the reference period 1986-2005

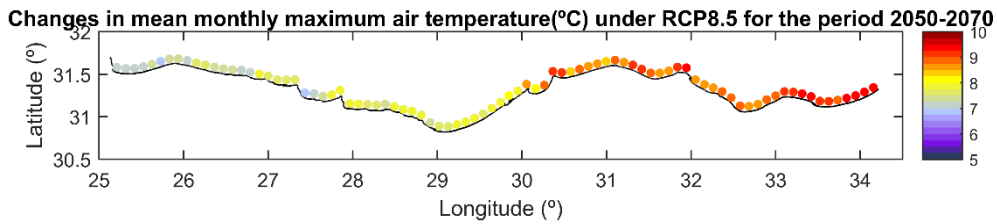


Fig. 59 Changes in the mean value of the monthly maximum air temperature (°C) under RCP8.5 for the period 2050-2070 with respect to the reference period 1986-2005

### 3.6. Precipitation: CMIP5 (spatial resolution: 1°)

Precipitation projections have been assembled using the results given by the CMIP5 models at a spatial resolution of 1° (Taylor et al., 2012). The following figures show changes in the monthly mean value of precipitation during the dry and the wet season (April to September and October to March, respectively) for the RCP4.5 and RCP8.5 emission scenarios, and for the periods 2030-2040 and 2050-2070 with respect to the reference period 1986-2005.

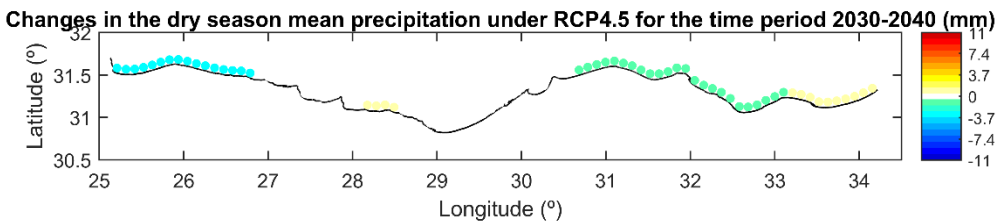


Fig. 54 Changes in the monthly mean value of precipitation (mm) during the dry season (April to September) under RCP4.5 for the period 2030-2040 with respect to the reference period 1986-2005

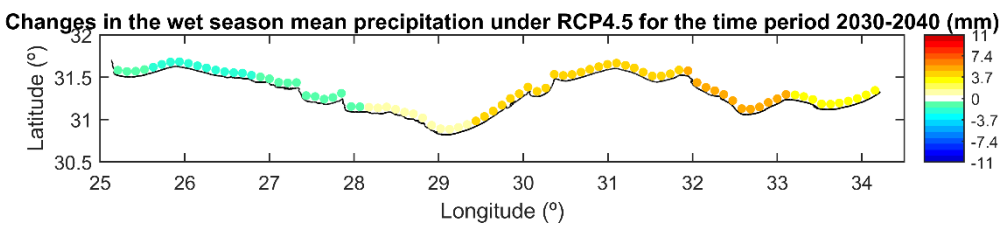


Fig. 55 Changes in the monthly mean value of precipitation (mm) during the wet season (October to March) under RCP4.5 for the period 2030-2040 with respect to the reference period 1986-2005

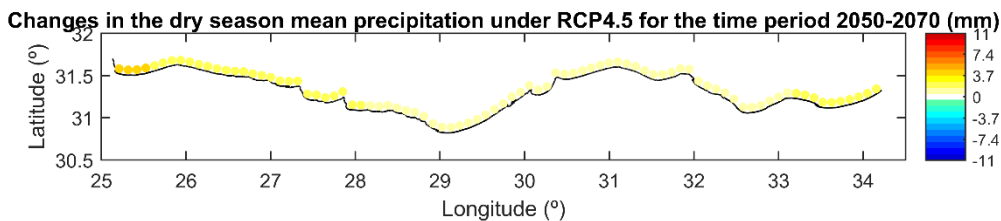


Fig. 56 Changes in the monthly mean value of precipitation (mm) during the dry season (April to September) under RCP4.5 for the period 2050-2070 with respect to the reference period 1986-2005



Fig. 57 Changes in the monthly mean value of precipitation (mm) during the wet season (October to March) under RCP4.5 for the period 2030-2040 with respect to the reference period 1986-2005

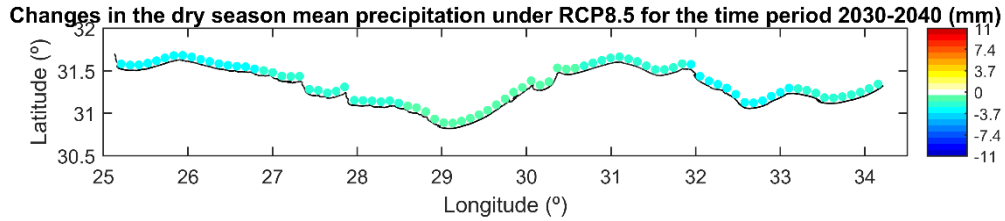


Fig. 58 Changes in the monthly mean value of precipitation (mm) during the dry season (April to September) under RCP8.5 for the period 2030-2040 with respect to the reference period 1986-2005

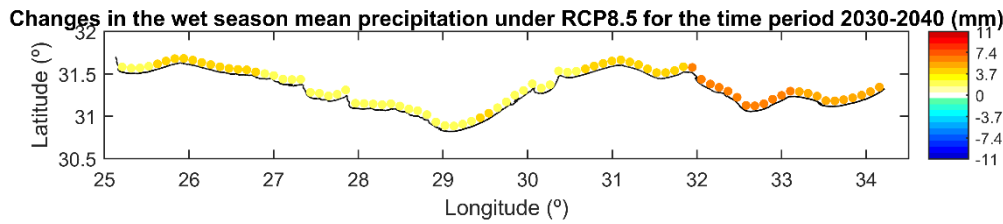


Fig. 59 Changes in the monthly mean value of precipitation (mm) during the wet season (October to March) under RCP8.5 for the period 2030-2040 with respect to the reference period 1986-2005

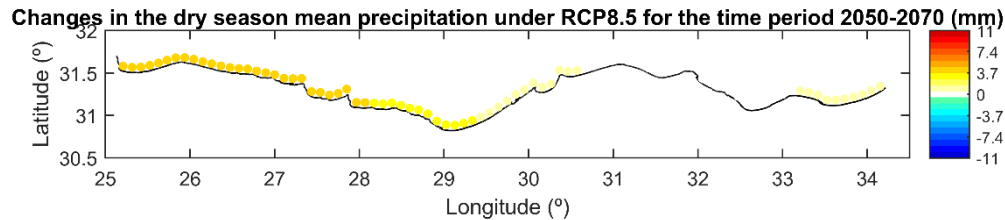


Fig. 60 Changes in the monthly mean value of precipitation (mm) during the dry season (April to September) under RCP8.5 for the period 2050-2070 with respect to the reference period 1986-2005

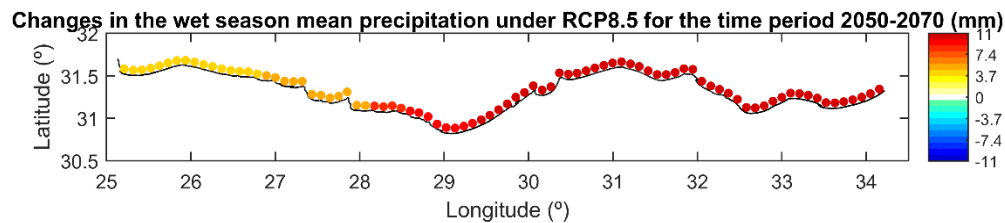


Fig. 61 Changes in the monthly mean value of precipitation (mm) during the wet season (October to March) under RCP8.5 for the period 2050-2070 with respect to the reference period 1986-2005

#### 4. REFERENCES

- Cid A, Castanedo S, Abascal AJ, Menéndez M, Medina R (2014) A high resolution hindcast of the meteorological sea level component for Southern Europe: the GOS dataset. *Clim Dyn*, doi: 10.1007/s00382-013-2041-0.
- Church JA, Clark PU, Cazenave A et al (2013) Sea Level Change. In: *Climate Change 2013: The Physical Science Basis. Contribution of Working Group I to the Fifth Assessment Report of the Intergovernmental Panel on Climate Change* [Stocker TF, Qin D, Plattner G-K et al (eds.)]. Cambridge University Press, Cambridge, United Kingdom and New York, NY, USA.
- Donlon, CJ, Martin M, Stark J, Roberts-Jones J, Fiedler E, Wimmer W (2012) The operational sea surface temperature and sea ice analysis (OSTIA) system: *Remote Sensing of Environment*, 116, 140-158.
- Global Historical Climatology Network – Daily: <https://www.ncdc.noaa.gov/oa/climate/ghcn-daily/>
- IPCC (2013) Summary for policymakers. In: *Climate Change 2013: The Physical Science Basis. Contribution of Working Group I to the Fifth Assessment Report of the Intergovernmental Panel on Climate Change* [Stocker TF, Qin D, Plattner G-K, Tignor M, Allen SK, Boschung J, Nauels A, Xia Y, Bex V and Midgley PM (eds.)]. Cambridge University Press, Cambridge, United Kingdom and New York, NY, USA.
- Perez J, Menéndez M, Camus P, Méndez FJ, Losada IJ (2015). Statistical multi-model climate projections of surface ocean waves in Europe. *Ocean Modelling*, doi:10.1016/j.ocemod.2015.06.001.
- Reguero BG, Menéndez M, Méndez FJ, Mínguez R, Losada IJ (2012). A Global Ocean Wave (GOW) calibrated reanalysis from 1948 onwards. *Coastal Engineering* 65 (2012) 38–55.
- Roberts-Jones J, Fiedler EK, Martin MJ (2012). Daily, Global, High-Resolution SST and Sea Ice Reanalysis for 1985–2007 Using the OSTIA System: *J. Climate*, 25, 6215–6232.
- Slangen ABA., Carson M, Katsman CA, Van de Wal RSW, Köhl A, Vermeersen LLA, Stammer D (2014) Modelling twenty-first century regional sea-level changes. *Climatic Change*, doi:10.1007/s10584-014-1080-9.
- Taylor KE, Stouffer RJ, Meehl GA (2012) An Overview of CMIP5 and the Experiment Design. *Bull Amer Meteor Soc* 93: 485–498.

